J. Fluid Mech. (1992), *vol.* 243, *pp.* 595–622
Printed in Great Britain

Fine-scale turbulence structure of intermittent shear flows

By V. R. KUZNETSOV[1], A. A. PRASKOVSKY[2] AND V. A. SABELNIKOV[2]

[1] Central Institute of Aviation Motors, 2, Aviamotornaya, Moscow, 111250, Russia
[2] Central Aero-Hydrodynamical Institute, Zhukovsky-3, Moscow region, 140160, Russia

(Received 20 March 1990 and in revised form 9 April 1992)

An experimental investigation of the fine-scale structure of turbulence was carried out. Five different shear flows were studied: three in a wind tunnel with an open working section and an elliptical nozzle and two in a wind tunnel of closed working section and square cross-section. The experiments tested two approaches to the theory of fine-scale turbulence structure: one based on the Navier–Stokes equations and the other on some similarity hypotheses. The variability of all fine-scale constants (including exponents in inertial-subrange power laws and the Kolmogorov constant) is revealed. A correlation between all fine-scale constants and the external intermittency coefficient is established.

1. Introduction

Modern considerations concerning the fine-scale structure of turbulence at high Reynolds numbers are based on the theory which was proposed by Kolmogorov (1941) and Oboukhov (1941). They assumed that there was no direct interaction between large energy-containing eddies and small energy-dissipating ones, but rather a cascade of energy from larger to smaller scales in the spectrum of turbulence. At large Reynolds numbers the number of steps in such a cascade is also large. As a result some kind of universal equilibrium of small eddies can be expected. This means that the fine-scale structure of turbulence depends on a few parameters only. Originally, it was assumed that only the mean dissipation $\bar{\epsilon}$ was essential. In this case the well-known equation

$$\overline{\Delta u^2} = \overline{[u(x+r)-u(x)]^2} = C(\bar{\epsilon}r)^{\frac{2}{3}} \tag{1}$$

is valid for inertial-subrange turbulence ($\eta \ll r \ll L$). Here u is a longitudinal velocity fluctuation, x is a longitudinal coordinate, r is a distance between two points, C is the Kolmogorov constant, $\eta = (\nu^3/\bar{\epsilon})^{\frac{1}{4}}$ is the Kolmogorov lengthscale, ϵ is the dissipation rate, ν is the kinematic viscosity, and L is the integral turbulence lengthscale defined as

$$L = \frac{U}{u^2}\int_0^\infty \overline{u(t+t_1)\,u(t)}\,\mathrm{d}t_1$$

assuming the validity of Taylor's hypothesis since only flows with low turbulence intensity ($(u^2)^{\frac{1}{2}}/U \ll 1$) will be considered below. Here U is the mean longitudinal velocity, t is time.

Equation (1) has been confirmed many times (see for instance the review by Yaglom 1981). However, it was found in many experiments that the original theory is not valid for high-order moments of the velocity difference Δu (see Monin &

Yaglom 1967). This is due to the large variability of the instantaneous dissipation field, which is often called 'internal intermittency'. In particular it was found that

$$R_{\epsilon\epsilon} = \overline{\epsilon(x)\,\epsilon(x+r)} = C_\epsilon \bar{\epsilon}^2 (L/r)^\mu, \tag{2}$$

if $\eta \ll r \ll L$. Here C_ϵ and μ are also inertial-subrange constants. It is assumed (Monin & Yaglom 1967) that (2) is valid down to scales of the order of η, i.e.

$$\overline{\epsilon^2} = R_{\epsilon\epsilon}(0) \sim \bar{\epsilon}^2 (L/\eta)^\mu.$$

Therefore the r.m.s. dissipation fluctuation is a growing function of the Reynolds number.

The influence of internal intermittency on fine-scale statistics has been studied by Kolmogorov (1962), Oboukhov (1962), Novikov & Stewart (1964), Yaglom (1966), Novikov (1971) and many others. Since the various expressions for high-order moments are different only in minor details, it is convenient to consider a similarity hypothesis which was proposed by Kolmogorov (1962) and slightly refined by Kuznetsov (1976).

Consider three points $\boldsymbol{x}^{(1)}$, $\boldsymbol{x}^{(2)}$, $\boldsymbol{x}^{(3)}$ such that $\eta \ll r \equiv |\boldsymbol{x}^{(2)} - \boldsymbol{x}^{(1)}| \ll R \equiv |\boldsymbol{x}^{(3)} - \boldsymbol{x}^{(1)}| \ll L$, i.e. two inertial-subrange eddies with a large difference in length-scales. According to the original Kolmogorov (1962) hypothesis the conditional p.d.f. of velocity differences $\boldsymbol{v} = \boldsymbol{u}(\boldsymbol{x}^{(2)}) - \boldsymbol{u}(\boldsymbol{x}^{(1)})$ (assuming the velocity difference $\boldsymbol{V} = \boldsymbol{u}(\boldsymbol{x}^{(3)}) - \boldsymbol{u}(\boldsymbol{x}^{(1)})$ to be constant) depends only on $\boldsymbol{v}, \boldsymbol{r}, \boldsymbol{V}, \boldsymbol{R}$. If turbulence is locally isotropic, large-eddy orientation (i.e. orientation of vectors $\boldsymbol{V}$ and $\boldsymbol{R}$) is insignificant. Therefore the conditional p.d.f. of the velocity difference $\boldsymbol{v}$ depends only on two vectors ($\boldsymbol{v}$ and $\boldsymbol{r}$) and two scalars ($|\boldsymbol{V}|$ and $|\boldsymbol{R}|$). An exact relation

$$\overline{\Delta u^n} \sim r^{q(n)} \tag{3}$$

can be derived from this similarity hypothesis (Kuznetsov 1976; Kuznetsov & Sabelnikov 1986). Here $q(n)$ is some unknown function, which cannot be derived from the similarity considerations.

We have $q = \frac{1}{3}n$ if the original Kolmogorov (1941) theory is valid. At the present time two models are the most popular. The first one, the 'lognormal' model, was proposed by Kolmogorov (1962) and Oboukhov (1962), and yields

$$q(n) = (\tfrac{1}{3} + \tfrac{1}{6}\mu)\, n - \tfrac{1}{18}\mu n^2. \tag{4}$$

The second, β-model, was originally proposed by Novikov & Stewart (1964). Later it was analysed in more detail by Frisch, Sulem & Nelkin (1978). Here we have

$$q(n) = \mu + \tfrac{1}{3}(1-\mu)\, n. \tag{5}$$

The equation

$$\mu = 2 - q(6) \tag{6}$$

was proposed by Monin & Yaglom (1967), Kuznetsov (1976) and Frisch *et al.* (1978). It is based on dimensional considerations. Let us consider the correlation $\overline{\epsilon(\boldsymbol{x})\,\epsilon(\boldsymbol{x}+\boldsymbol{r})}_v$ which is obtained by averaging over time intervals when the condition $v_0 < |\boldsymbol{v}| < v_0 + \mathrm{d}v$ is met. We have

$$\overline{\epsilon(\boldsymbol{x})\,\epsilon(\boldsymbol{x}+\boldsymbol{r})}_v = \text{const.} \times v_0^6 / r^2$$

if there is no dependence on the Reynolds number. It is evident that

$$R_{\epsilon\epsilon} = \int \overline{\epsilon(\boldsymbol{x})\,\epsilon(\boldsymbol{x}+\boldsymbol{r})}_v P\,\mathrm{d}v = \text{const.} \times v^6 / r^2 \sim r^{q(6)-2},$$

where P is the p.d.f. of velocity differences.

Both (4) and (5) predict $q(2) \approx \frac{2}{3}$ since $\mu \approx 0.2$ (see for instance the review of Kuznetsov & Sabelnikov 1986). Thus (1) is approximately valid.

It seems that one important question remains unresolved: is the function $q(n)$ the same under all flow conditions?

The answer would be affirmative if the similarity hypothesis has been stated correctly. In this case there are no additional parameters governing the fine-scale structure of turbulence. If the answer is negative, then there are some additional governing parameters, i.e. generally speaking the function $q(n)$ would be different in various flows or various locations of the same flow.

At the present time there is a large amount of data concerning the exponent μ in (2) (see reviews by Monin & Yaglom 1967 and Kuznetsov & Sabelnikov 1986). However, most of the data were not taken systematically, i.e. only one measurement is reported in each article; the scatter is rather large ($0.2 < \mu < 0.5$). This could be attributed in part to the lack of measurement accuracy (for more discussion see §4). On the other hand, large and systematic variations of the exponent μ were observed in our preliminary experiments (Kuznetsov, Praskovsky & Sabelnikov 1984, 1988). It is worth noting also that there is rather large variability of other inertial-subrange constants. For instance a large variation in the Kolmogorov constant C has been observed ($1.6 < C < 2.5$); see for example reviews by Monin & Yaglom (1967), Yaglom (1981) and Kuznetsov & Sabelnikov (1986). Such a variability is larger than the accuracy of measurements, which is about 10% (see for instance Champagne 1978). There are also two quite different theoretical considerations suggesting the variability of the inertial-subrange constants (see the next section).

These considerations stimulated us to perform systematic measurements of various fine-scale characteristics in five different shear flows. The main purpose of this study was to find out if there is a variability of inertial-subrange constants.

2. Theoretical background

Our experiments were based on the following theoretical considerations. It is convenient to begin with the more familiar one, which is related to basic ideas of multifractal theory (Parisi & Frisch 1985) where the exponent μ and other exponents in inertial-subrange power laws are treated as random variables. Equation (2) should be modified now to

$$R_{\varepsilon\varepsilon} \sim \int \left(\frac{r}{L}\right)^{-\mu} P(\mu)\,\mathrm{d}\mu,$$

where $P(\mu)$ is the p.d.f. of the exponent μ. Equation (2) remains approximately valid in the double limit $r/L \to 0$, $\eta/r \to 0$.

We have

$$R_{\varepsilon\varepsilon} \sim \int^{\mu_{\max}} \exp\left(\mu \ln \frac{L}{r}\right) P(\mu)\,\mathrm{d}\mu \approx P(\mu_{\max}) \left(\frac{r}{L}\right)^{-\mu_{\max}} \frac{1}{\ln (L/r)} \tag{7}$$

since $\ln (L/r) \gg 1$. Here $\mu_{\max}$ is a maximum value of μ. It is easily seen that (7) differs from (2) only by a slowly varying correction factor $1/\ln (L/r)$.

It is assumed that the random variation of each exponent is caused by the singularities of solutions of the inviscid Navier–Stokes equations, i.e. different values of each exponent correspond to the different types of singularities. Since this consideration is based on the intrinsic properties of dynamic equations, it could be

expected that the statistics of each exponent does not depend on particular flow conditions.

Some work has been done to verify the Parisi–Frisch model. However, most of the data were obtained using the measurements of conventionally averaged moments (see for instance Chhabra *et al.* 1989). The interpretation of these data is not straightforward since all conventionally averaged moments could be well approximated by power laws and such an approximation would be valid if there is no random variability of inertial subrange exponents. Some work has been done to find singularities directly from velocity time histories (Argoul *et al.* 1989, Bacry *et al.* 1989). In our opinion, the results were inconclusive.

The second theoretical consideration is based on the equation for the p.d.f. of the velocity difference $P(\boldsymbol{v}, r)$ (Kuznetsov 1976, see also Kuznetsov & Sabelnikov 1986). The pressure term in this equation is equal to some integral over phase space $(\boldsymbol{V}, \boldsymbol{R})$ and the integrand is proportional to the p.d.f. $P(\boldsymbol{v}, \boldsymbol{r}, \boldsymbol{V}, \boldsymbol{R})$ of the two velocity differences $\boldsymbol{v}$ and $\boldsymbol{V}$, i.e. the equation for $P(\boldsymbol{v}, \boldsymbol{r})$ is not closed. However, one important conclusion could be drawn from the similarity hypothesis alone. We found, after long and complicated analytical work, that the large-scale contribution to the pressure term (i.e. the role of scales which are much larger than r) is insignificant only if

$$q(n)-q(n-2) < 2. \tag{8}$$

It is evident that inequality (8) is valid for all values of n if the original Kolmogorov (1941) model ($q = \frac{1}{3}n$) or the β-model, (5), are used. In other cases the inequality (8) could be violated at some n, i.e. there is a direct interaction between eddies with a large difference of lengthscales. Thus it could be expected that the function $q(n)$ depends on the structure of the largest eddies. If their characteristics are random functions, then it could be expected that $q(n)$ would be also random. Therefore both theoretical considerations suggest the random variability of all exponents in inertial-subrange power laws. However, the cause of such a variability is quite different in the second case since the role of boundary conditions in the formation of the largest eddies is important. Thus it could be expected that all exponents (including a maximum value of μ as is defined by (2)) are different in various flows or even in various locations of the same flow, if there is a direct interaction between eddies with large difference of lengthscales. This conclusion could be easily verified by relatively unsophisticated experiments. It seems also that the proof of the random variability of exponents could be based on measurements of the quantity $\epsilon(x)\epsilon(x+r)$ conditionally averaged under some (not yet known) conditions. If the exponent μ depends on the conditions imposed, this would be proof of its random variability.

There are several reasons to study the influence of external intermittency on the variability of exponent μ. This phenomenon occurs at any free-stream edge – in boundary layers as well as in jets and wakes. It is caused by random movement of the boundary dividing the outside part of a flow, where no vorticity is present (non-turbulent fluid), and the inner part of a flow where violent vorticity fluctuations (turbulent fluid) exist (Townsend 1956). Internal intermittency is met only in the turbulent part of the flow. It is often assumed that internal and external intermittency are quite different phenomena (Chhabra *et al.* 1989).

However, it is not easy to make a clear distinction between the effects of the two types of intermittency (Kuznetsov & Sabelnikov 1976, ch. 1). It is evident that vorticity (and hence dissipation) is not zero through the entire flow field (except at some points) if the Reynolds number R is finite. Thus for the quantitative definition

of external intermittency it is necessary to adopt some threshold level, ϵ_0, assuming that fluid is turbulent if $\epsilon > \epsilon_0$ and non-turbulent otherwise. However, there is no satisfactory method of selecting ϵ_0. One would think that this difficulty could be overcome if the Reynolds number is made infinite since it can be assumed that $\epsilon_0 = 0$. A new difficulty is encountered in this case. It is caused by the finite resolution of any experimental device (if experiments are performed) or numerical code (if Navier–Stokes simulations are done). Therefore one can measure or calculate only a dissipation ϵ^l averaged over some volume of size l. Thus the external intermittency factor γ should be defined as

$$\gamma = \lim_{\substack{l \to 0 \\ \epsilon_0 \to 0 \\ R \to \infty}} \text{prob}\,(\epsilon^l > \epsilon_0). \tag{9}$$

As was mentioned in §1 the r.m.s. dissipation fluctuation is infinitely large at infinite Reynolds number. Therefore the choice of l would influence ϵ^l significantly if l is small and the Reynolds number is large but finite. Hence there is a possibility that the limit (equation (9)) does not exist, as was suggested by Kuznetsov & Sabelnikov (1986). Such a possibility was also suggested by our preliminary experiments (for more discussion see §5).

Thus it is convenient to adopt a more general definition of external intermittency: it will be assumed that external intermittency exists if there are regions of non-zero volume where the energy dissipation rate tends to zero in the limit of infinite Reynolds number. This means that γ is equal to the upper limit in (9).

There are some considerations indication that $\gamma < 1$ at all locations of all flows, based on the equation for the p.d.f. of passive scalar concentration (Kuznetsov 1967, 1972; Kuznetsov & Sabelnikov 1986). To close this equation it was assumed that concentration and scalar dissipation were statistically independent quantities (see also the report of Kuznetsov & Raschupkin 1977 where this assumption was verified). This assumption is an extension of Batchelor's (1953) hypothesis about the statistical independence of Fourier modes with large difference of wavenumbers. As shown by Batchelor (1953), it is based on a cascade mechanism of energy transfer in the turbulence spectrum, i.e. it is one of the most important conclusions of Kolmogorov theory.

It was proved that the external intermittency factor γ is always less than unity, i.e. an external intermittency is observed everywhere. Of course, this does not necessarily mean that intermittency is considerable everywhere. For instance $1-\gamma \sim 10^{-4}$ at the round jet axis, which is well beyond measurement accuracy.

As was pointed out by Kuznetsov & Sabelnikov (1986, ch. 3) the existence of external intermittency (in the sense of the definition in (9)) is a rather strict consequence of Kolmogorov (1941) theory. This was the main reason for studying the influence of the external intermittency factor on the value of inertial-subrange constants. Some other models also suggest the existence of such an influence. For instance it was assumed in a multifractal model of Siebesma *et al.* (1989) that the probability of eddy fragmentation depends on the activity of neighbouring regions. This would imply that the exponent μ is a function of γ.

Since variability of the inertial-subrange constants was found in our preliminary experiments (Kuznetsov *et al.* 1984, 1988) it becomes evident that (1) and (2) are approximations which are valid only if the effects of external intermittency are small. Its possible generalization could be based on a highly simplified model, i.e. it would be assumed that turbulent and non-turbulent volumes could be separated quite easily, which is possible only if the scales of external and internal intermittency

are quite different. It is evident that the universal equilibrium of small eddies could be expected only within a turbulent fluid, i.e.

$$\overline{\Delta u_t^2} = C_t(\bar{\epsilon}_t r)^{\frac{2}{3}}, \quad \overline{\epsilon_t(x)\,\epsilon_t(x+r)} = C_{\epsilon t}\bar{\epsilon}_t^2\,(L/r)^{\mu_t}, \tag{10}$$

where subscript t denotes a conditional averaging over turbulent fluid and C_t, $C_{\epsilon t}$, μ_t are new quantities expected to be universal constants.

Equations for conventionally averaged quantities could be derived from (10). It is convenient to define an intermittency function $\Gamma(x)$ such that $\Gamma = 1$ if $\epsilon(x) > 0$ and $\Gamma = 0$ otherwise. There are four possibilities, i.e. both points (x and $x+r$) are within the turbulent fluid, both points are within the non-turbulent fluid, the first point is within the turbulent fluid and the second point is within the non-turbulent fluid and vice versa. Let us denote the corresponding probabilities as γ_{tt}, γ_{nn}, γ_{tn} and γ_{nt}. For locally homogeneous turbulence we have (Kuznetsov & Sabelnikov 1986)

$$\gamma_{tt} = \gamma - \tfrac{1}{2}D_{\gamma\gamma}, \quad \gamma_{nn} = 1-\gamma-\tfrac{1}{2}D_{\gamma\gamma}, \quad \gamma_{nt} = \gamma_{tn} = D_{\gamma\gamma},$$

where

$$\gamma = \bar{\Gamma}, \quad D_{\gamma\gamma} = \overline{[\Gamma(x+r)-\Gamma(x)]^2}.$$

It is seen from these equations that $\gamma_{tt} \to \gamma$, $\gamma_{nn} \to 1-\gamma$, $\gamma_{nt} = \gamma_{tn} \to 0$ if $r \to 0$ since $D_{\gamma\gamma} \to 0$ if $r \to 0$. Thus only two possibilities need be considered if small-scale eddies are of major interest, i.e. both points are within a turbulent fluid or both points are within a non-turbulent fluid. It is well-known that small-scale fluctuations can be neglected in a non-turbulent fluid (Phillips 1955). Thus we have

$$\overline{\Delta u^2} = \gamma\overline{\Delta u_t^2} = \gamma^{\frac{1}{3}}C_t(\bar{\epsilon}_t r)^{\frac{2}{3}}, \quad R_{\epsilon\epsilon}^t = \gamma\overline{\epsilon_t(x)\,\epsilon_t(x+r)} = \gamma^{-1}C_{\epsilon t}\bar{\epsilon}_t^2(L/r)^{\mu_t},$$

i.e.

$$C = \gamma^{\frac{1}{3}}C_t, \quad C_\epsilon = \gamma^{-1}C_{\epsilon t}, \quad \mu = \mu_t. \tag{11a–c}$$

Here the relation $\bar{\epsilon} = \gamma\bar{\epsilon}_t$ has been used.

In spite of some shortcomings of the theoretical arguments it is evident now that the Kolmogorov constant C, defined by (1), can be a non-universal quantity. This conclusion is rather obvious. However, as far as we know it has neither been tested experimentally (except in our preliminary reports) nor taken into account in theoretical predictions. It should be kept in mind that the verification of analytical theories of turbulence is based mainly on the comparison between measured and calculated values of the Kolmogorov constant C. Apparently the variability of 'constant' C would contradict the theoretical results. However, only a slight modification of such theories is necessary if quantity C_t is a universal constant, i.e. these theories should be applied only to a turbulent fluid. This was the reason for testing (10) and (11).

It is seen from (11) that there is no direct (or, more precisely, kinematical) influence of intermittency on the exponent μ. As far as we know this conclusion has been tested only twice (Kuznetsov *et al.* 1984, 1988). It was not confirmed by these experiments, but there was some evidence suggesting that μ was a universal function of γ.

It seems that the observed variability of exponent μ is indirect evidence of direct interaction between the largest and the smallest eddies. Direct evidence of such an interaction could be obtained if two quantities are measured. The first one is defined as follows:

$$\overline{\left(\frac{\partial u}{\partial x}\right)_u^2} = \left\{\int\left(\frac{\partial u}{\partial x}\right)^2 P\left(u, \frac{\partial u}{\partial x}\right) d\left(\frac{\partial u}{\partial x}\right)\right\} \Big/ P(u), \tag{12}$$

where $P(u)$ is a p.d.f. of velocity, and $P(u, \partial u/\partial x)$ is the joint p.d.f. of the velocity and

its derivative. It is evident that this quantity does not depend on u if there is a big separation of scales between energy-containing and energy-dissipating eddies and there is no direct interaction between such eddies. It is worth noting that the hypothesis concerning the statistical independence of u and $(\partial u/\partial x)^2$ plays an important role in the derivation of the equation for the p.d.f. of velocity (Kuznetsov 1967) and in the derivation of corrections to hot-wire measurements in high-intensity turbulent flows (Lumley 1965; Heskestad 1965).

The second quantity is defined as follows:

$$\overline{\left(\frac{\partial u}{\partial x}\right)^2}_{\Delta u} = \left\{\int\left(\frac{\partial u}{\partial x}\right)^2 P\left(\Delta u, \frac{\partial u}{\partial x}\right) d\left(\frac{\partial u}{\partial x}\right)\right\} \Big/ P(\Delta u), \tag{13}$$

where $P(\Delta u)$ is the p.d.f. of the velocity difference, and $P(\Delta u, \partial u/\partial x)$ is the joint p.d.f. of the velocity difference and velocity derivative. Here $\Delta u = u(x+r) - u(x)$, where r is a variable parameter. This quantity is a measure of the direct interaction between energy-dissipating eddies and eddies which have a linear scale equal to r. It plays an important role in the derivation of the equation for the p.d.f. of the velocity difference (Kuznetsov 1976).

3. Test facilities and data processing

3.1. *Wind tunnels and characteristics of shear flows*

Two wind tunnels were used. The first one had an open working section and elliptical nozzle. The length of the working section was 24 m. The major axis of the ellipse was 24 m long and the minor one 14 m long. The free-stream turbulence intensity was 0.6–0.8 %. The second tunnel had a 4 m long closed working section with a square cross-section 1×1 m^2. The turbulence intensity was 0.02–0.04 %.

The first wind tunnel was used to investigate three shear flows. The first flow was the axisymmetric wake behind a 10 m long cylinder placed along the tunnel axis (see figure 1*a*). The cylinder diameter d was 0.975 m. The flow velocity U_0 was 10.3 m/s, so that the Reynolds number $R = U_0 d/\nu$ was 6.7×10^5. All measurements were done at $x/d = 16.8$, where x is the distance from the cylinder trailing edge.

The second flow was the wake behind the same cylinder placed symmetrically along the major axis of the nozzle (figure 1*b*). This flow could be called a three-dimensional wake since the cylinder length was less than the length of the major nozzle axis. Measurements were done along the minor axis of the cross-section located at distance $x/d = 19.7$ from the cylinder axis. The flow velocity U_0 was 9.89 m/s ($R = 6.4 \times 10^5$).

The third flow was the mixing layer between the jet issuing from the wind-tunnel nozzle and the ambient air. The jet velocity U_0 was 10.9 m/s. Measurements were performed at a distance $x = 20$ m from the nozzle ($R = U_0 x/\nu = 1.5 \times 10^7$). All data were taken in the high-speed part of the mixing layer.

The second wind-tunnel was used to investigate two other flows. The first was a plane two-dimensional wake behind a cylinder. Its diameter d was 5 cm. Flow velocity U_0 was 8.12 m/s ($R = 2.7 \times 10^4$). Measurements were done at distance $x/d = 58.6$ from the cylinder axis. The second flow was the boundary layer on the wind-tunnel wall. Flow velocity U_0 was 8.13 m/s and the boundary-layer thickness δ was 3.82 cm ($R = U_0 \delta/\nu = 2.1 \times 10^4$).

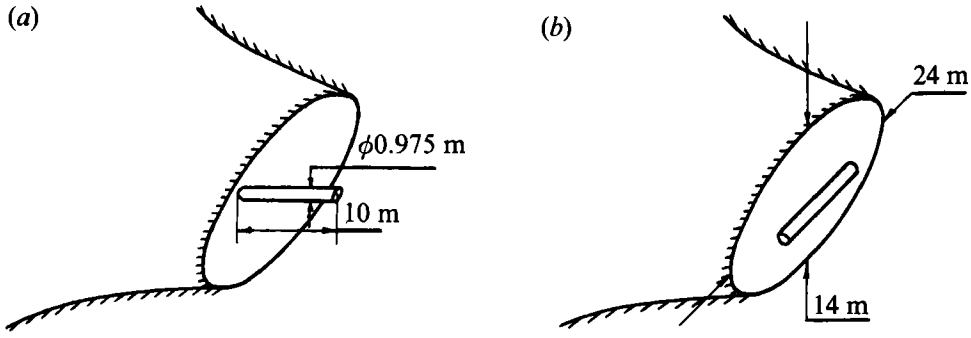

FIGURE 1. Location of test cylinders in the 24×14 m^2 tunnel nozzle.

3.2. *Measurements and data processing*

A single hot-wire made of platinum-plated tungsten and a constant-temperature anemometer (DISA 55A01) were used. The hot-wire was 0.33 mm long and its diameter was 2.2 μm. To check the spatial resolution some measurements were done with wires 1 and 3 mm long. A linearizer was not used since the turbulence intensity was quite low (see the next section).

A tape recorder (Schlumberger MP5522) was used to record the hot-wire signal. The tape velocity was equal to 38.1 cm/s, so that frequencies up to 10 kHz were resolved. As will be seen in the next subsection, the Kolmogorov frequency $f_K = U/2\pi\eta$ was everywhere less than 10 kHz.

Velocity realizations stored on a magnetic tape were digitized using as 12 bit analog-to-digital converter and processed on a digital computer. A low-pass filter was used at the digitizer input to reduce the noise level still further. The choice of its cutoff frequency was based on the following considerations. It was found that spectra of velocity derivatives obtained without a low-pass filter were growing functions of frequency if the frequency was more than about 8 kHz. It was found also that the Kolmogorov frequency was roughly the same in all experiments ($f_K \approx 3.5$–7.1 kHz). Thus it was natural to reduce the noise level by removing frequencies of more than 6.4 kHz. A similar procedure was used by Antonia, Satyaprakash & Hussain (1982).

A sampling frequency of $f_S = 32$ kHz was used, i.e. the ratio of discretization spatial interval $\Delta x = U\Delta t$ to the Kolmogorov scale η was equal to 0.7–1.3 ($\Delta t = 1/f_S$ is the discretization time interval). This ratio was better than is usually achieved (see for example Champagne, Pao & Wygnanski 1976 where it was about 2 for the central region of the mixing layer). Each quantity was averaged over a time interval equal to 53.25 s, i.e. 1704000 samples were stored. The influence of sampling interval on measured turbulence characteristics will be discussed in §4.

As will be seen later, the turbulence intensity was fairly low ($(\overline{u^2})^{\frac{1}{2}}/U = 0.03$–$0.11$) in all cases except at one location in the mixing layer. We therefore used Taylor's 'frozen flow' hypothesis, i.e. it was assumed that

$$r \equiv x^{(2)} - x^{(1)} = U(t^{(2)} - t^{(1)}), \quad \frac{\partial}{\partial x} = -\frac{1}{U}\frac{\partial}{\partial t}. \tag{14}$$

For more discussion see the next section.

Cubic splines as well as the equation

$$\frac{\partial u}{\partial x} = \frac{u(t+\Delta t) - u(t)}{2\Delta t}$$

Location	$\hat{y}$	U (m/s)	$(\overline{u^2})^{\frac{1}{2}}$ (m/s)	L (m)	$\bar{\epsilon}$ (m^2/s^3)	R_λ	η (mm)	f_K (kHz)	γ	$\bar{\epsilon}_t$ (m^2/s^3)	$\bar{\epsilon}_n$ (m^2/s^3)
AW1	0.685	9.39	0.668	0.445	0.270	860	0.33	4.5	0.46	0.721	0.033
AW2	1.02	9.75	0.571	0.462	0190	745	0.37	4.2	0.37	0.571	0.027
AW3	1.72	10.2	0.355	0.453	0.117	370	0.41	4.0	0.21	0.553	0.030
TW1	0	8.64	0.592	0.531	0.462	515	0.29	4.7	0.63	0.878	0.044
TW2	1.34	9.55	0.481	0.614	0.279	440	0.33	4.6	0.30	0.974	0.050
TW3	1.60	9.71	0.408	0.608	0.229	360	0.35	4.4	0.24	0.978	0.037
ML1	0.05	9.82	1.12	1.06	0.811	1400	0.25	6.2	0.52	1.81	0.181
ML2	0	7.30	1.51	1.14	1.88	1660	0.21	5.5	0.89	2.62	—
PW1	0	7.22	0.497	0.127	1.65	190	0.21	5.5	1.0	—	—
PW2	1.18	7.78	0.400	0.097	1.03	160	0.24	5.1	0.70	1.70	0.054
BL1	0.209	6.00	0.684	0.097	11.7	140	0.13	7.3	1.0	—	—
BL2	1.15	8.10	0.179	0.283	0.189	75	0.37	3.5	0.10	1.16	0.083

TABLE 1. Turbulence characteristics at the locations studied in detail. AW and TW denote locations in the axisymmetric and three-dimensional wakes, ML in the mixing layer, PW in the plane wake and BL in the boundary layer. The numeral after each abbreviation corresponds to the location number in a particular flow.

were used to calculate the velocity derivative. The results agreed to within 0.1% for the r.m.s. velocity derivative.

Local isotropy was assumed in order to calculate C and μ, i.e. it was assumed that

$$\bar{\epsilon} = 15\nu\overline{(\partial u/\partial x)^2}. \tag{15}$$

The errors produced by this assumption will be discussed in §6,

The equation

$$R_{\epsilon\epsilon}(r) = \left[\frac{\partial u(x)}{\partial x}\frac{\partial u(x+r)}{\partial x}\right]^2 = C_\epsilon\overline{\left(\frac{\partial u}{\partial x}\right)^2}\left(\frac{L}{r}\right)^\mu \tag{16}$$

was used instead of (2) to calculate C_ϵ and μ. It is evident that value of the exponent μ given by (2) and (16) would be the same for isotropic or nearly isotropic turbulence.

To characterize the flow regimes, two lengthscales were used. The first was the integral lengthscale L defined in §1. The second was the Taylor microscale

$$\lambda = (\overline{u^2}/\overline{(\partial u/\partial x)^2})^{\frac{1}{2}}$$

This scale was used to define the Reynolds number

$$R_\lambda = \frac{(\overline{u^2})^{\frac{1}{2}}\lambda}{\nu}.$$

3.3. *Flow regimes*

Quantities C, C_ϵ and μ were measured at many locations in all five flows. To gain more detailed information two or three locations were chosen in each flow. As a rule the chosen locations represent regions with the smallest and the largest external intermittency. Detailed information concerning turbulence characteristics at these locations is presented in table 1. Locations in the axisymmetric and three-dimensional wakes, the mixing layer, the plane wake and the boundary layer are included. The lateral coordinate y was non-dimensionalized, i.e. $\hat{y} = y/\delta$ for all wakes and the boundary layer, and $\hat{y} = y/x$ for the mixing layer. Here δ is a wake half-width or boundary-layer thickness.

It is seen that rather large Reynolds number R_λ (up to 1700), low turbulence intensity (less than 0.11), high spatial resolution (with one exception hot-wire length was less than 1.6η), high temporal resolution (the Kolmogorov frequency $f_K = U/2\pi\eta$ was below the cut-off frequency, 6.4 kHz) were achieved.

4. Accuracy of measurements

4.1. *The accuracy of inertial-subrange approximations*

It was convenient to calculate the one-dimensional spectrum E_1 instead of the structure function $\overline{\Delta u^2}$. It is known (see Monin & Yaglom 1967) that

$$E_1(k) = \frac{1}{\pi}\int_0^\infty \overline{u(x)\,u(x+r)}\cos(kr)\,\mathrm{d}r = C_1\bar{\epsilon}^{\frac{2}{3}}k^{-\frac{5}{3}}, \quad C_1 = C/4.02 \tag{17}$$

in the inertial subrange. Here $k = 2\pi f/U$ is a wavenumber.

Some data are presented in figure 2. In all cases constant C_1 was calculated using the least-squares method. It was found that (17) is valid to within $\pm 5\%$ accuracy. In some cases the constant C was calculated from (1): the difference between calculations based on (1) and (17) was not more than a few percent.

Four methods were used to calculate the exponent μ. The first was based on (16), and the second on the quantity

$$B_{\epsilon\epsilon}(r) = R_{\epsilon\epsilon}(r) - \left[\overline{\left(\frac{\partial u}{\partial x}\right)^2}\right]^2, \tag{18}$$

which is almost equal to $R_{\epsilon\epsilon}$ if $r/L \to 0$ and $\eta/r \to 0$ (see (2)).

The third was based on a Fourier transform of (18), i.e.

$$E_{\epsilon\epsilon} = \frac{1}{2\pi}\int_0^\infty B_{\epsilon\epsilon}(r)\cos(kr)\,\mathrm{d}r \sim k^{1-\mu}; \tag{19}$$

and the fourth was based on (6). All methods would be identical if the Reynolds number were high enough.

It was proved that power-law approximations were good in all cases. As an example, tests of the validity of power-law approximations are presented in figure 3. However, it was found that exponents μ measured by various methods are different, even in a mixing layer where the Reynolds number was as high as $R_\lambda = 1700$. At the location ML2, $\mu = 0.14$ from (16); $\mu = 0.45$ from (18); $\mu = 0.60$ from (19) and $\mu = 0.24$ from (6).

It should be emphasized that (16) and other similar equations are valid only asymptotically (Reynolds number tends to infinity and distance r tends to zero). Therefore other terms in the asymptotic (16) could be important if the variation of the first term within an inertial subrange is not large. Perhaps this was the case since the ratio of values of $R_{\epsilon\epsilon}$ at the lower and the upper bounds of the inertial subrange did not exceed 3. Of course, this consideration is also valid for the second-order structure function and one-dimensional spectrum. However, it is less important there since the variation of turbulence spectrum across the inertial subrange was more than two orders of magnitude.

Since other terms in expansion (16) are not known yet, there are no theoretical arguments to help decide on the best definition of exponent μ, nor is there any possibility of measuring it at a sufficiently higher Reynolds number. The highest reported Reynolds number was about $R_\lambda = 13000$ (Champagne 1978), which seems

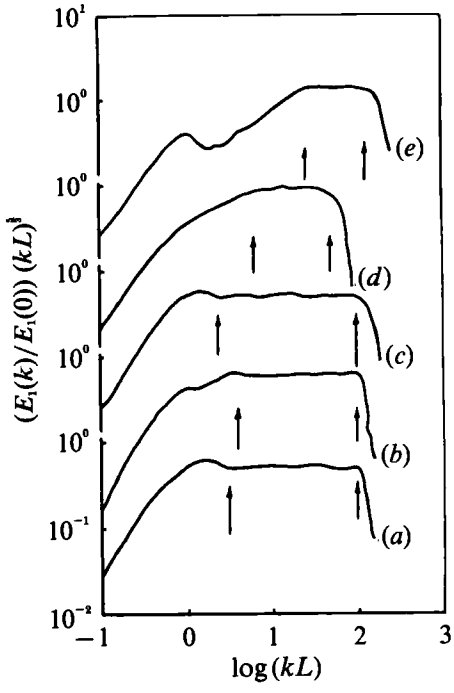

FIGURE 2. Velocity spectra in various flows. Vertical arrows denote the boundaries of the inertial subrange. (*a*) AW3; (*b*) TW2; (*c*) ML2; (*d*) PW2; (*e*) BL2.

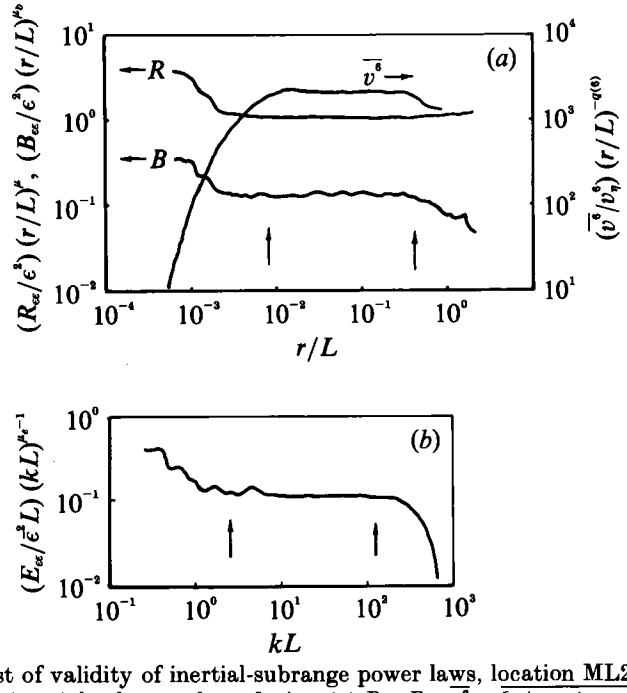

FIGURE 3. A test of validity of inertial-subrange power laws, location ML2. Vertical arrows denote the inertial-subrange boundaries. (*a*) $R_{\varepsilon\varepsilon}$, $B_{\varepsilon\varepsilon}$, $\overline{v^6} = \overline{[u(x+r)-u(x)]^6}$; (*b*) $E_{\varepsilon\varepsilon}$.

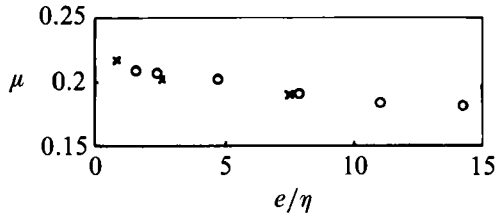

FIGURE 4. The influence of spatial resolution on measured values of exponent μ, location AW3: ×, hot wires of different lengths; ○, numerical averaging.

to be close to the highest possible. In Champagne's measurements the length of the inertial subrange was up to three decades (compared to two decades in the present data). It is easily seen that the variation of $R_{\epsilon\epsilon}$ within an inertial subrange would not be large even at $R_\lambda = 13000$ (it would be about a factor six if $\mu = 0.25$).

Therefore the definition of exponent μ adopted here was somewhat arbitrary: it was based on (16). A similar definition is widely used now (see Antonia *et al.* 1982). There was only one justification: it is seen in figure that the power-law approximation is good enough. Surprisingly this approximation is valid well beyond the upper boundary of the inertial subrange (up to $r \approx L$).

4.2. *The spatial resolution*

As seen in table 1, the ratio of hot-wire length to the Kolmogorov scale was equal to 2.5 in the worst case. Thus it could be concluded from the results of Wyngaard (1968) that the accuracy of mean dissipation measurements was better than 4% if no other sources of errors were present. However, the influence of spatial resolution on the measurement accuracy needs more attention since we are interested in measuring the second moment of the dissipation. In this case the role of dissipation fluctuations is expected to be large, since the instantaneous value of the Kolmogorov scale (i.e. $\eta = (\nu^3/\epsilon)^{\frac{1}{4}}$) could be low.

Since Wyngaard's theory could not be applied in this case it was decided to perform two experiments. Additional measurements with hot wires of length 1 and 3 mm were made in the first experiment. The idea of the second experiment was based on Wyngaard's data. It was shown that the signal from a hotwire is equal to the velocity averaged over its length. Therefore the signal registered by a hotwire of length 0.33 mm was averaged over a variable time interval.

Some data are presented in figure 4. It is seen that the extrapolation of data down to zero hot-wire length would lead to negligible corrections. It is seen also that the observed exponent μ decreases when the spatial resolution becomes poorer. The same results were obtained in other flows. The trend observed by Pond & Stewart (1965) was the opposite.

It could also be concluded that the influence of the ratio of hot-wire length to its diameter (which was slightly less than usual) is negligible. The influence of spatial resolution on the accuracy of measurements of constants C and C_ϵ was studied in the same experiments. It was found to be about 5%.

4.3. *Nonlinearity of hot-wire response and Taylor's hypothesis*

As was mentioned above, the turbulence intensity was quite low, i.e. the nonlinearity of the hot-wire response and corrections to Taylor's hypothesis could be neglected. On the other hand the influence of these factors on the measured value of exponent μ should be analysed, since this exponent is expected to be small. For simplicity it

is convenient to consider a one-dimensional model. Write the relation between measured velocity w and true velocity u as $w = f(u)$. We have

$$\frac{\partial w}{\partial t} = f'(u)\frac{\partial u}{\partial t},$$

$$\left(\frac{\partial w}{\partial t}\frac{\partial w_1}{\partial t_1}\right)^2 = [f'(u)f'(u_1)]^2\left(\frac{\partial u}{\partial t}\frac{\partial u_1}{\partial t_1}\right)^2, \tag{20}$$

where subscript 1 denotes the velocity at time t_1. Now Heskestad's (1965) assumption

$$\frac{\partial}{\partial t} = -(U+u)\frac{\partial}{\partial x} \tag{21}$$

can be used. Combining (20) and (21) we obtain

$$\left(\frac{\partial w}{\partial t}\frac{\partial w_1}{\partial t_1}\right)^2 = [f'(u)f'(u_1)]^2(U+u)^2(U+u_1)^2\left(\frac{\partial u}{\partial t}\frac{\partial u_1}{\partial t_1}\right)^2. \tag{22}$$

It can be assumed that $f(u) \approx f(u_1)$, $U+u_1 \approx U+u$ since the correlation $R_{\epsilon\epsilon}$ is calculated in an inertial subrange where the difference $t-t_1$ is small. It can also be assumed that the velocity and its gradient are statistically independent quantities. This assumption will be proved in §7. Thus we have from (22)

$$\overline{\left(\frac{\partial w}{\partial t}\frac{\partial w_1}{\partial t_1}\right)^2} = \overline{[(U+y)f'(u)]^2}R_{\epsilon\epsilon}.$$

In other words the nonlinearity of the hot-wire response and corrections to Taylor's hypothesis could affect only the constant C_ϵ and there is no influence of either factor on the exponent μ. The proof would be the same in a three-dimensional case.

4.4. *Instrumentation errors*

The signal-to-noise ratio was measured in the free stream of the first wind tunnel. The mean flow velocity was approximately the same for all five flows, as listed in table 1 ($U_0 \approx 10$ m/s). The signal-to-noise ratio was 25–250 for velocity fluctuations and 5–20 for velocity derivative fluctuations.

4.5. *Convergence of various moments*

As can be seen in table 1, the ratio of turbulence integral time scale L/U to the sampling interval T was largest at location ML2. Therefore this location was chosen to study the convergence of various moments. We have used the data of Champagne *et al.* (1976) which were also obtained in a mixing layer. It was assumed that the convergence of all moments depended only on the non-dimensional quantity UT/x. It was found that the sampling interval should be equal to $T = 3$ min to gain 5% accuracy in the velocity variance and should be equal to $T = 45$ min to gain the same accuracy in dissipation measurements.

Since the sampling interval was too large in the latter case, it was decided to study the convergence of non-dimensional quantities such as

$$C = \frac{\overline{\Delta u^2}}{(\bar{\epsilon}r)^{\frac{2}{3}}}, \quad C_\epsilon = \frac{R_{\epsilon\epsilon}}{\bar{\epsilon}^2(r/L)^\mu}, \tag{23}$$

which were the most important in providing information about the variability of the inertial-subrange constants. Note that all quantities in (23) were averaged over the same time interval. Theoretical considerations indicate that the statistics of the

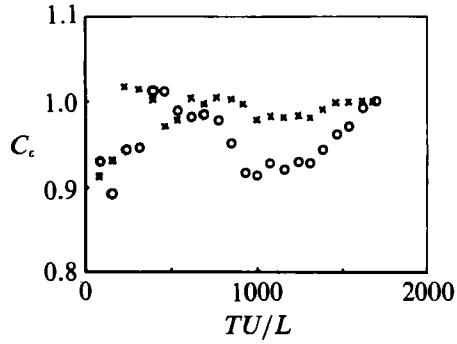

FIGURE 5. The influence of sampling interval on constant C_ϵ; all data are taken at $r/\eta = 59.5$, location ML2: ×, dissipation averaged over a variable time interval; ○, dissipation averaged over time interval of 5 min.

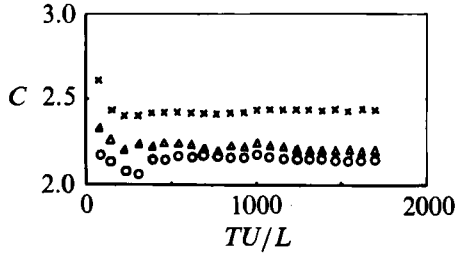

FIGURE 6. The influence of sampling interval on constant C, location ML2. Dissipation has been averaged over a variable time interval: ○, $r/\eta = 59.5$; ×, 316; △, 1780.

velocity difference $\Delta u(r)$ depends only on the dissipation averaged over a space interval equal to r (Oboukhov 1962). Therefore it could be expected that the convergence of non-dimensional quantities defined by (23) would be better than convergence of $\overline{\Delta u^2}$ and $R_{\epsilon\epsilon}$.

This was the case. One example for the constant C_ϵ is given in figure 5. Note that the sampling interval at this location was five times longer than that indicated in §4 ($T = 5$ min). It was found that the maximum difference between values of C_ϵ obtained for $T = 1$ and 5 min was about 10%. This difference is small compared with the total variation of correlation $R_{\epsilon\epsilon}$ within an inertial subrange (it was about three times). Convergence of the Kolmogorov constant was better than convergence of constant C_ϵ (see figure 6). The maximum difference between values of C obtained for $T = 1$ and 5 min was about 5%.

5. External intermittency measurements

Strictly speaking, intermittency measurements must be performed with a vorticity meter. Existing devices are combinations of several hot wires which are packed within a volume with linear size of the order of 1.5–3 mm (Antonia, Browne & Shah 1988; Foss & Wallace 1989; Tsinober, Kit & Dracos 1992). It is seen in table 1 that these devices could resolve scales which are larger than 5η–15η, i.e. the spatial resolution would be poor. Therefore it was decided to use a longitudinal velocity derivative as a detector.

As is seen from reviews by Hedley & Keffer (1974), Antonia (1981) and Praskovsky (1982), intermittency measurements are based on the generation of an intermittency function Γ which is equal to 1 if a detection function g is above some threshold level

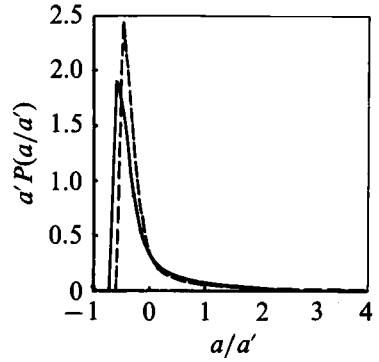

FIGURE 7. P.d.f. of velocity derivative modulus $a = |\partial u/\partial t| - \overline{|\partial u/\partial t|}$, $a' = (\overline{a^2})^{\frac{1}{2}}$. ——, location TW3; – – –, BL2.

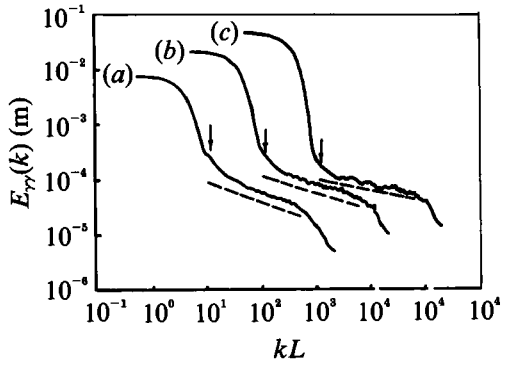

FIGURE 8. Spectra of the intermittency function at location AW2 obtained at different threshold levels. Solid lines denote experimental data, dotted lines denote inertial-subrange power laws, vertical arrows denote mean turbulent interval. Note the one order-of-magnitude shift for curve (*b*) and two orders-of-magnitude shift for curve (*c*) along the abscissa. (*a*) $h/[\overline{(\partial u/\partial x)^2}]^{\frac{1}{2}} = 2.26$, $\gamma = 0.178$, $\zeta = 0.37$; (*b*) $h/[\overline{(\partial u/\partial x)^2}]^{\frac{1}{2}} = 1.18$, $\gamma = 0.372$, $\zeta = 0.30$; (*c*) $h/[\overline{(\partial u/\partial x)^2}]^{\frac{1}{2}} = 0.60$, $\gamma = 0.619$, $\zeta = 0.21$.

h during a time interval more than τ, and is equal to zero otherwise. Usually $g = (\partial u/\partial t)^2$ or $g = |\partial u/\partial t|$ if a single hot wire is used. Various modifications of such a method were tried in the present work since we found considerable difficulties which could not have been anticipated from existing data obtained at moderate Reynolds numbers. The first difficulty is clearly seen in figure 7 where the p.d.f. of the velocity derivative modulus is presented. There is no preferable threshold level. The second difficulty will become clear after an examination of the intermittency function spectrum $E_{\gamma\gamma}$.

To calculate this spectrum, the detection function was chosen to be $g = |\partial u/\partial t|$. It has been smoothed by a digital low-pass filter with cut-off frequency equal to $f_F = \frac{1}{8} f_K$, i.e. it was equal to the frequency where the maximum of the dissipation spectrum was observed. Such a smoothing was equivalent to choosing $\tau = 1/2\pi f_F$. Thus all viscous scales were removed.

Spectra of the intermittency function are presented in figure 8. The threshold level h was varied here: in all cases it was chosen to satisfy a condition $\bar{\epsilon}_t \gg \bar{\epsilon}_n$ where subscripts t and n denote conditional averaging over turbulent and non-turbulent fluid respectively. In particular it was found that $\bar{\epsilon}_t/\bar{\epsilon}_n = 21$ for curve (*b*), obtained with a threshold level defined later in this section.

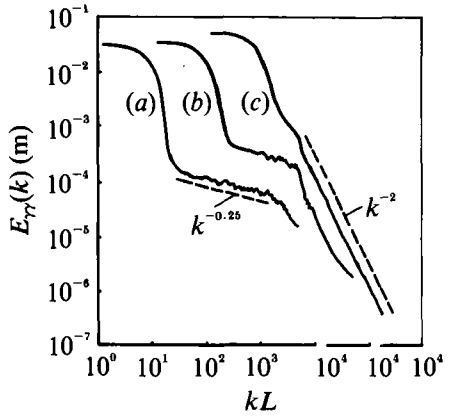

FIGURE 9. The influence of smoothing at location ML1. Note the one order-of-magnitude shift for curve (*b*) and two order-of-magnitude shift for curve (*c*) along abscissa. (*a*) $f_F/f_K = 10/8$; (*b*) 1/8; (*c*) 1/80.

Two clearly distinguishable regions are seen in figure 8, for $k < 1/L_t$ and $k > 1/L_t$. Here L_t is a mean turbulent interval which is equal to $x_i - x_{i-1}$, where x_i is a leading edge of the intermittency function and x_{i-1} is a trailing edge of the intermittency function ($\Gamma = 1$ if $x_i < x < x_{i-1}$). It is evident that the second high wavenumber region is a typical inertial subrange where the intermittency function spectrum could be approximated as follows:

$$E_{\gamma\gamma}(k) = Ak^{-\zeta}. \tag{24}$$

Here constant A does not depend on k. This is something quite new since this subrange is absent at moderate Reynolds numbers (see for instance LaRue & Libby 1976). To model moderate-Reynolds-number data, the detection function was smoothed still further (see figure 9). No inertial subrange is seen with large smoothing. Smoothed data are the same as those of LaRue & Libby (1976), i.e.

$$E_{\gamma\gamma}(k) \sim k^{-2}$$

if the wavenumber is sufficiently large. It is also seen that the spectrum of the intermittency function and hence the intermittency factor is influenced significantly by the value of the cutoff wavenumber.

It seems that the large-scale part ($k < 1/L_t$) of the intermittency spectrum is caused by the external intermittency and the small-scale part ($k > 1/L_t$) of the spectrum is caused by the internal intermittency. The transition between both parts is rather abrupt. Hence the model leading to (10) and (11) seems to be correct, as least qualitatively. However, it is very difficult to draw quantitative conclusions about the external intermittency, since we have from (24)

$$\gamma = \int_0^\infty E_{\gamma\gamma}\,\mathrm{d}k \approx \int_0^{1/\eta} E_{\gamma\gamma}\,\mathrm{d}k = \int_0^{1/L_t} E_{\gamma\gamma}\,\mathrm{d}k + \int_{1/L_t}^{1/\eta} E_{\gamma\gamma}\,\mathrm{d}k = B + \frac{A}{1-\zeta}\eta^{\zeta-1}, \tag{25}$$

where the constant B does not depend on η. It could be concluded that the constant A tends to zero at infinite Reynolds number since $\gamma < 1$ and $\zeta < 1$ in all cases, i.e. the spectrum of intermittency function in an inertial subrange depends significantly on Reynolds number.

It is evident from the previous discussion that an inertial subrange of the intermittency function spectrum would not be present at infinite Reynolds number since $A \to 0$. However, the term $A\eta^{\zeta-1}$ in (25) could be either zero or non-zero at

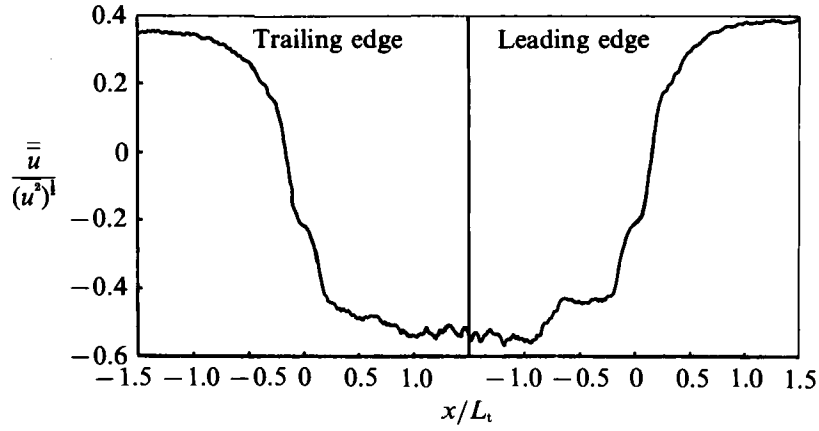

FIGURE 10. Conditionally averaged velocity in the vicinity of the boundary between turbulent and non-turbulent fluid, location AW2.

infinite Reynolds number. The second case is quite possible, as was found from the integration of spectra presented in figure 8 ($\gamma = 0.13$ for curve a, $\gamma = 0.26$ for curve b, $\gamma = 0.44$ for curve c if wavenumbers larger than $1/L_t$ were removed). It is clear that the overall intermittency factor is of the same order of magnitude (see the caption to figure 8). Of course definite conclusions could only be drawn from measurements at much higher Reynolds numbers. However, that would be very difficult since the Reynolds numbers reported here are close to the maximum value that can be obtained in laboratory.

It was also found that the exponent ζ in (24) depends on the threshold level. Hence it is quite probable that the limit (9) does not exist, as was discussed in §2.

Therefore the intermittency factor described below should be treated as an empirical correlation parameter. The resulting values of this parameter are close to the usual external intermittency factor since we have used a method proposed by Townsend (1956), i.e. it was assumed that the kurtosis of the velocity derivative K_t is constant within a turbulent fluid. As was mentioned earlier, the detector function was chosen to be $g = |\partial u/\partial t|$. It was smoothed by a low-pass digital filter with cutoff frequency $\frac{1}{8}f_K$. It is evident that one empirical constant (i.e. K_t) needs to be found to use Townsend's method. Usually it could be measured in the region where external intermittency is negligible. However, such measurements were impossible in the mixing layer, at the axisymmetric and three-dimensional wakes since considerable intermittency was found throughout these flows. (It must be noted that the intermittency factor is always significantly less than unity in the mixing layer. This was also the case in some of the wakes studied, since measurements were done at a moderate distance from a cylinder). Therefore it was decided to adopt some empirical equation for the threshold level. Plane wake data were used for this purpose since no intermittency was found on the plane of symmetry. The threshold level was assumed to be

$$h = z(\gamma)\left(\overline{\left(\frac{\partial u}{\partial t}\right)^2}_n\right)^{\frac{1}{2}}.$$

An empirical function

$$z(\gamma) = 1.2(1-\gamma^4)^{\frac{1}{2}}$$

was chosen to produce the best agreement between the adopted method and Townsend's method. Since the threshold level was not known *a priori* several iterations were needed to generate an intermittency function.

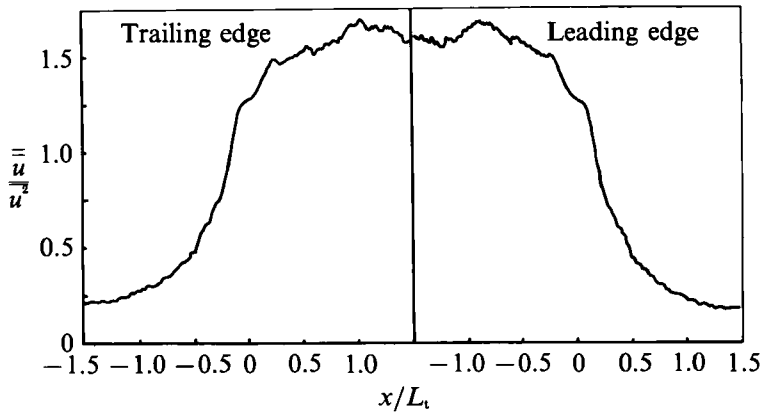

FIGURE 11. Conditionally averaged velocity fluctuation in the vicinity of the boundary between turbulent and non-turbulent fluid, location AW2.

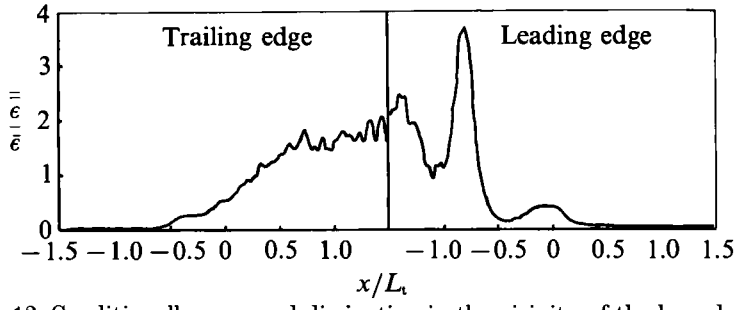

FIGURE 12. Conditionally averaged dissipation in the vicinity of the boundary between turbulent and non-turbulent fluid, location AW2.

In all cases the value of $\overline{(\partial u/\partial t)_n^2}$ averaged over non-turbulent fluid was much less than that averaged over turbulent fluid (see table 1). To investigate further whether or not a reasonable threshold level was chosen, the flow conditions in the vicinity of the interface between turbulent and non-turbulent fluid have been studied. Two sequences: $t_i^{(1)}$ ($\Gamma(t_i^{(1)}-0)=0$, $\Gamma(t_i^{(1)}+0)=1$) and $t_i^{(2)}$ ($\Gamma(t_i^{(2)}-0)=1$, $\Gamma(t_i^{(2)}+0)=0$) were selected, i.e. the trailing and leading edges of intermittency function were studied separately. Velocity, turbulence energy and mean-square velocity derivative were averaged overall $t_i^{(1)}$ or $t_i^{(2)}$ for the conditions $t-t_i^{(1)}=$ const or $t-t_i^{(2)}=$ const, where $|t-t_i^{(1)}|$ or $|t-t_i^{(2)}|$ were less than a half the turbulent time interval. Such an averaging is denoted by a double overbar.

Results are presented in figures 10–12: considerable variations of all quantities across the interface are clearly seen. Similar results were reported by Jenkins & Goldschmidt (1976). Thus it seems that the choice of threshold level was reasonable. Of course this is not a very reliable proof, and therefore the method adopted here gives only a rough estimate of the external intermittency factor.

6. Inertial-subrange constants

6.1. *Kolmogorov constant*

Measurements of the Kolmogorov constant C are presented *vs.* the intermittency factor in figure 13. It is seen that (11*a*) is confirmed by the present data.

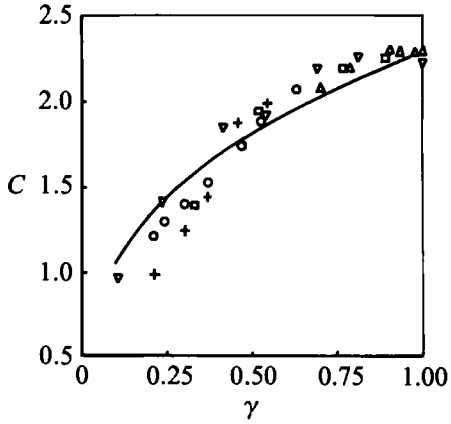

FIGURE 13. The influence of intermittency factor on the Kolmogorov constant. solid line corresponds to the power law $C \sim \gamma^{\frac{1}{3}}$: +, AW; ○, TW; □, ML; △, PW; ▽, BL.

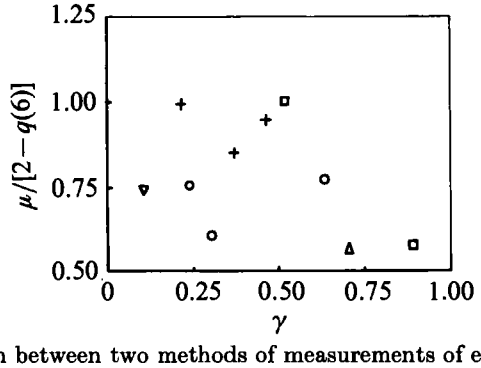

FIGURE 14. A comparison between two methods of measurements of exponent μ. For symbols see figure 13.

However, some uncertainties must be kept in mind. There are some doubts concerning (15) since it is valid only if the fine-scale structure is isotropic. Moreover, the degree of anisotropy could be different at various locations. For instance the dissipation, calculated from (15), is 45% less than the true value at the wake plane of symmetry and is 80% less than the true value at the wake edge (Browne, Antonia & Shah 1987). Therefore the true experimental curve $C(\gamma)$ would be steeper than the experimental curve shown in figure 13. There are also some uncertainties concerning the measurements of intermittency.

6.2. *Exponent* μ

Four methods were used to calculate exponent μ (see §3.1). It was shown that values of μ given by different methods are different. One more example is given in figure 14. Here μ was calculated from (16), and a good correlation was found between μ in (16) and the intermittency factor (see figure 15). There are two new findings. The first one is the variability of exponent μ. This conclusion does not depend on the definition of the intermittency factor or on its measurement inaccuracy. The second finding is the universal dependence of μ on γ. This is relatively unimportant since this 'universality' has of course been demonstrated only for the flows actually studied (see discussion §8). Thus universality should be treated only as a proof of the systematic variation of exponent μ. Hence one can conclude that errors in measuring μ are relatively unimportant.

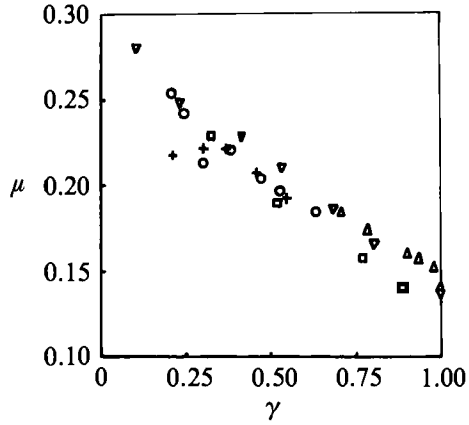

FIGURE 15. The influence of intermittency factor on exponent μ. For symbols see figure 13.

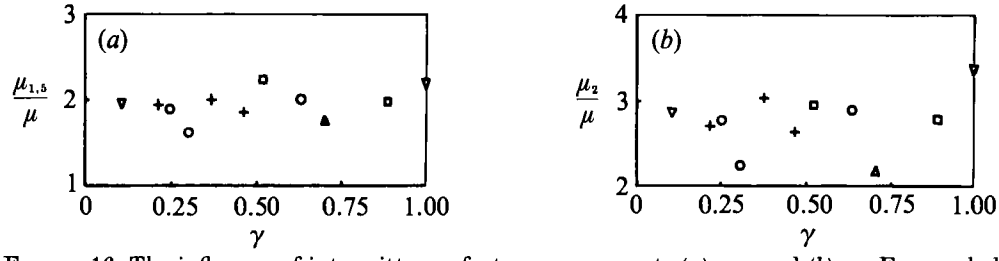

FIGURE 16. The influence of intermittency factor on exponents (*a*) $\mu_{1.5}$ and (*b*) μ_2. For symbols see figure 13.

To give more proof that variability of the inertial-subrange exponents does exist, the quantities

$$R_n(r) = \overline{\left[\frac{\partial u(x)}{\partial x}\frac{\partial u(x+r)}{\partial x}\right]^{2n}}$$

were calculated for $n = 1.5, 2$. It was found that data could be well approximated by the equation

$$R_n(r) \sim r^{-\mu_n} \tag{26}$$

if an inertial subrange was considered. Since similar results were reported by Gagne & Hopfinger (1979), a comparison between (26) and experimental data is not presented. Equation (26) is not trivial, since correlations $R_n(0)$ and $R_n(\infty)$ $(n \neq 1)$ depend quite differently on Reynolds number (Monin & Yaglom 1967). Thus an influence of Reynolds number could be expected even if an inertial subrange is considered. Generally speaking, power laws such as given by (26) are not valid for $n > 1$.

Data for $n = 1.5$ and 2 are presented in figure 16. These data are somewhat lower than those of Gagne & Hopfinger (1979) ($\mu_{1.5} \approx \frac{2}{3}$, $\mu_2 \approx \frac{5}{6}$). It is seen in figure 16 that $\mu_{1.5}/\mu \approx$ const and $\mu_2/\mu \approx$ const. Since μ is a universal function of γ this means that both exponents are also universal functions of γ. It is also seen that exponent μ_2 is up to three times larger than exponent $\mu_1 \equiv \mu$. Exponent $\mu_{1.5}$ is also larger than μ. Therefore correlations $R_{1.5}$ and R_2 vary more rapidly with r than R_{ee} does (it was

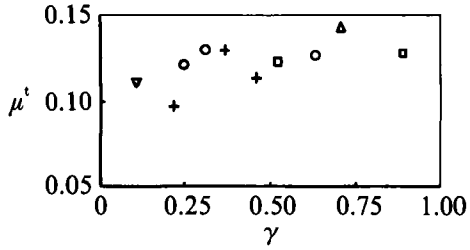

FIGURE 17. The influence of intermittency factor on exponent μ^t. For symbols see figure 13.

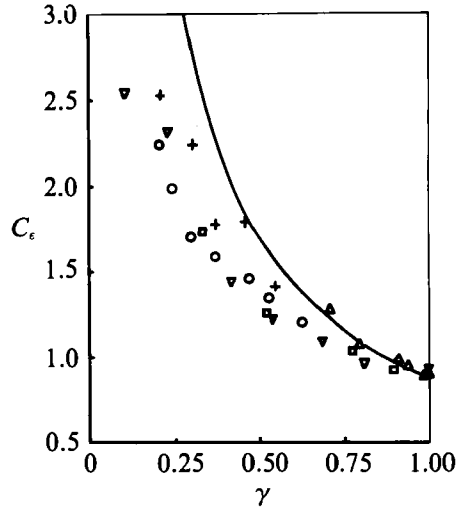

FIGURE 18. The influence of intermittency factor on the constant C_ϵ. Solid line denotes the power law $C_\epsilon \sim \gamma^{-1}$. For symbols see figure 13.

found that R_2 varies by a factor of about 30 in an inertial subrange). Thus it could be expected that the measurements of exponents $\mu_{1.5}$ and μ_2 were more accurate than the measurements of the small exponent μ_1, i.e. the correlation presented on figure 15 is not mere coincidence.

An additional experiment has been carried out to prove the variability of μ. As was explained in §1 this proof could be based on conditional averaging. Therefore the quantity $[\partial u(x)/\partial x\,\partial u(x+r)/\partial x]^2$ was averaged over all turbulent intervals which were longer than L_t. The exponent μ obtained by this conditional averaging is denoted by μ^t. Results are presented in figure 17. It is seen that μ^t is considerably less than μ. It is also seen that the variability of exponent μ^t is less than the variability of μ. However, the accuracy of these measurements was not high enough since exponent μ^t was too small.

6.3. *Constant* C_ϵ

Good correlation was found between constant C_ϵ and the intermittency factor (see figure 18). Equation (16) was used to calculate these data. Equation (11*b*) was confirmed only qualitatively; quantitative agreement was not very good, probably due to the lack of accuracy of intermittency measurements. This lack of accuracy does not affect the correlation presented in figure 13 since the Kolmogorov constant is proportional to a small power of γ.

Constant C_ϵ was also calculated using conditional averaging over turbulent

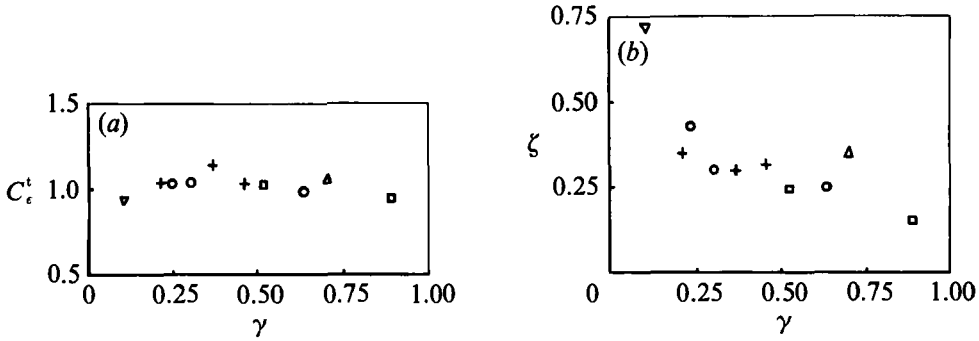

FIGURE 19. The influence of intermittency factor on (*a*) the constant C_ϵ^t and (*b*) the exponent ζ. For symbols see figure 13.

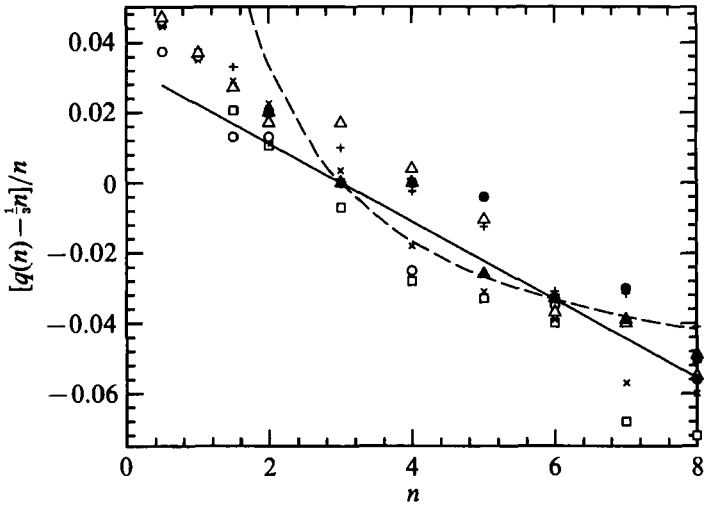

FIGURE 20. The test of validity of the lognormal and β-models. Present data: △, AW1; ○, AW3; □, TW1; +, ML1; ×, ML2; Data by Anselmet *et al.* (1984): ■, duct ($R_\lambda = 515$); ▲, jet ($R_\lambda = 536$); ●, jet ($R_\lambda = 852$). ——, Lognormal model; – – –, β-model (both with $\mu = 0.2$).

intervals which were longer than L_t. This version of the constant is denoted by C_ϵ^t. Results are presented in figure 19(*a*), and it is seen that C_ϵ^t does not depend on γ. This agrees with data presented in figure 17.

6.4. *Exponent ζ in equation* (24)

It was found that the exponent ζ in the inertial-subrange power law for the intermittency spectrum also depends on the external intermittency factor (see figure 19*b*). This dependence was approximately the same in all flows.

6.5. *Moments of various orders*

Quantities $\overline{|\Delta u(r)|^n}$ were calculated for $n = \frac{1}{8}$ up to $n = 8$. Power laws given by (3) were verified. The upper and lower bounds of the inertial subrange were approximately the same as for $n = 2$. Data are presented in figure 20. Results of Anselmet *et al.* (1984) obtained in a fully developed turbulent duct flow and in an axisymmetric jet are also presented in figure 20. It can be seen that the current results agree with those of Anselmet *et al.* (1984) within the data scatter. It seems

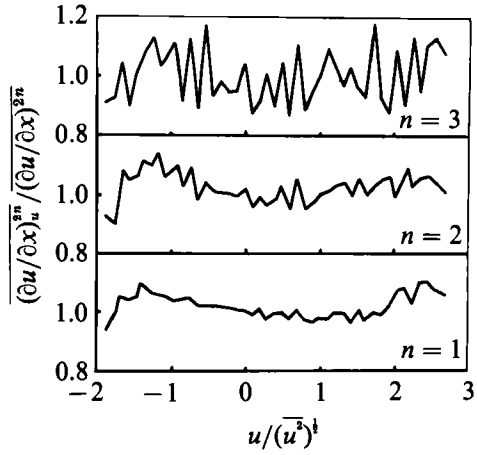

FIGURE 21. Various powers of dissipation conditionally averaged at a constant velocity, location PW1. Note the negligible intermittency.

that the lognormal model (4) provides a slightly better approximation than the β-model (5). However, the data scatter is rather large and it is a bit premature to draw a definite conclusion.

7. Measurements of conditionally averaged dissipation

Experiments reported in §6 suggest the variability of all inertial-subrange constants. It is likely that this is consequence of some direct interaction between small-scale and large-scale eddies, so it was natural to detect such an interaction in the measurements of the dissipation averaged at various conditions (see (12) and (13)). To calculate the quantity defined by (12), the square of velocity derivative was averaged over time intervals t_i and $t_i+\Delta t_i$, where $u(t_i)=u$ and $u(t_i+\Delta t_i)=u+\Delta u$. The velocity interval was equal to $\Delta u = 0.1\ (\overline{u^2})^{\frac{1}{2}}$. The same procedure was used to calculate

$$\overline{\left(\frac{\partial u}{\partial x}\right)_u^{2n}} = \left\{\int\left(\frac{\partial u}{\partial x}\right)^{2n} P\left(u, \frac{\partial u}{\partial x}\right) d\left(\frac{\partial u}{\partial x}\right)\right\} \Big/ P(u)$$

which is similar to that defined by (12).

No appreciable statistical dependence between the velocity and its derivative was found in the regions of negligible external intermittency (see figure 21). Similar results were obtained by Kuznetsov & Rasschupkin (1977), Praskovsky (1983) and Kuznetsov *et al.* (1984) at the plane of symmetry in a wake.

On the other hand there was a statistical dependence between the velocity and its derivative in the intermittent regions (see figure 22). However, such a dependence was not observed in a turbulent fluid (also see figure 22). To calculate the conditionally averaged velocity derivative squared $\overline{(\partial u/\partial x)^2_{u,t}}$ only turbulent intervals were considered. Other details of the calculation were the same as those reported above. Similar results were reported by Praskovsky (1983) and Kuznetsov *et al.* (1984).

The quantity defined by (13) was also calculated. The velocity derivative squared was averaged over time intervals t_i, $t_i+\Delta t_i$ such that

$$u(t_i)-u(t_i+r/U)=\Delta u, \quad u(t_i+\Delta t_i)-u(t_i+\Delta t_i+r/U)=\Delta u+\delta\Delta u,$$

where $\delta\Delta u = 0.1\ (\overline{\Delta u^2})^{\frac{1}{2}}$, $\Delta u = u(x+r)-u(x)$.

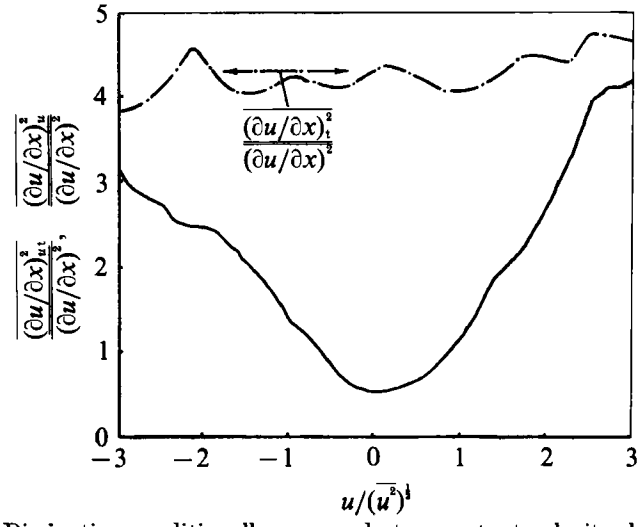

FIGURE 22. Dissipation conditionally averaged at a constant velocity, location TW3. —·—, $\overline{(\partial u/\partial x)^2_{u,t}}/\overline{(\partial u/\partial x)^2}$; ——, $\overline{(\partial u/\partial x)^2_u}/\overline{(\partial u/\partial x)^2}$.

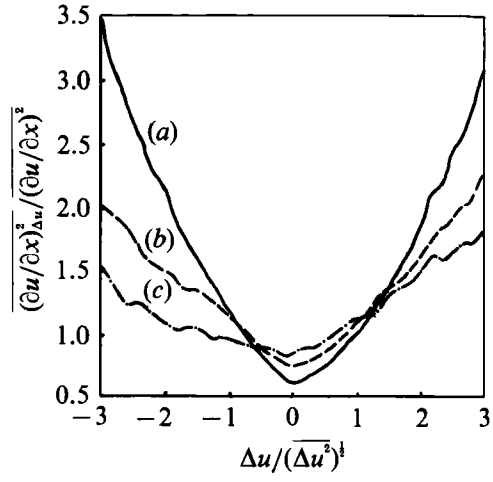

FIGURE 23. Dissipation conditionally averaged at a constant velocity difference, location ML2. (*a*) $r/L = 0.0103$, (*b*) 0.0515; (*c*) 0.257.

Some data are presented in figure 23. The statistical relation between fluctuations of dissipation and velocity differences is strongly pronounced at small r. Similar data were obtained in other cases.

It should be kept in mind that data presented in figures 22 and 23 were obtained in three-dimensional wakes where turbulence intensity was as low as 4.5% (see table 1). Therefore the use of Taylor's hypothesis for the calculation of velocity derivatives was adequate. Nonlinearity of hot-wire response was also negligible.

It seems that the independence of velocity and dissipation fluctuations is a manifestation of some equilibrium of turbulence fine-scale structure. Therefore such an equilibrium does not exist in an intermittent flow. On the other hand, some kind

of equilibrium does exist inside a turbulent fluid since velocity and dissipation at one point of this fluid are independent. However this equilibrium is not complete since there is a statistical relation between dissipation and the two-point velocity difference.

8. Discussion

The experiments reported herein were performed to test two approaches to the theory of fine-scale turbulence structure. There are many versions of the first approach (DIA, EQDNM and so on). All these versions are based on the Navier–Stokes equations and their goal is to predict the turbulence spectrum or the second-order structure function. Neither external nor internal intermittency is taken into account. The validation of this approach is based mainly on a comparison between measured and calculated values of the Kolmogorov constant. The second approach is based on some similarity hypotheses instead of the Navier–Stokes equations. Its main goal is to predict the influence of internal intermittency on the structure functions of various orders. External intermittency is not taken into account here either.

In contrast to the conclusion of the first approach, experiments reported prove the variability of the Kolmogorov constant beyond all doubt. The observed variability was up to a factor 2.5 (see figure 13); that is, much more than likely error of measurements. In an attempt to adopt classical results, a simple model leading to (10) was designed. It is based on three assumptions: (i) the variability of the Kolmogorov constant is caused by an external intermittency; (ii) there is a distinct boundary between turbulent and non-turbulent fluid; (iii) the fine-scale properties of turbulent fluid are the same in all flows. The validity of these assumptions for the prediction of the second-order structure function was verified since there was good agreement between data and (10) (see figure 13). Therefore it seems that there would be no difficulties if the first approach (based on the Navier–Stokes equations) were applied to the turbulent fluid.

However, some doubts still remain since there is a variation of other inertial-subrange constants (μ, $\mu_{1.5}$ and μ_2). These variation of the exponent μ was considerable (up to a factor two, see figure 15). Moreover, identical and systematic variation of these constants was observed in five different flows (see figures 15 and 16). Thus it seems that the variability of the inertial-subrange exponents was also proven. Hence the use of assumption (iii) leads to some errors and such errors are small only for the low-order moments. It should also be kept in mind that we were not able to make a clear distinction between effects caused by external and internal intermittency. This is a basic and yet unresolved difficulty. Moreover we do not know if there is a distinct boundary between turbulent and non-turbulent fluid. It is clear that the first approach should be basically modified if this is the case.

It seems that the variability of the exponents contradicts the second approach also, since it indicates that there are some other parameters which are not listed in the formulation of the similarity hypothesis. This is a key question concerning the whole of turbulence theory. The difficulty here is caused by the large number of degrees of freedom, mostly associated with the fine-scale motion. Thus a solution is possible if there is some universal equilibrium of small eddies and the dependence between fine-scale and large-scale statistics is established. It was assumed in the original Kolmogorov (1941) theory that fine-scale statistics depends only on $\bar{\epsilon}$. Since this theory was not completely successful one more quantity (i.e. the turbulence

integral scale) was added to the list of governing parameters. Now we see that this list is incomplete.

Hence it seems that variability of all inertial-subrange constants is the most important finding of the present work. It is clear that such variability depends neither on the definition of external intermittency nor on errors of measurements. The universal dependence of the inertial-subrange constants (see figures 13, 15 and 16) is a less important finding for two reasons. The first is the unsatisfactory definition of γ. Hence at the present time we do not know the influence of Reynolds number, large-eddy structure, etc. on the external intermittency factor.

The second reason is more complicated. To clarify it let us consider the wake behind a cylinder placed in a slowly fluctuating external flow with a non-zero lateral velocity. Let us assume that the scale of external fluctuations is much larger than the distance between the cylinder and the cross-section where measurements are done. This flow could be modelled by the wake behind a cylinder randomly moved in a lateral direction. Let the position of the cylinder axis y_0 be a stationary function of time, and let the integral timescale of this function be very large. It is clear that slow cylinder movement does not affect turbulence dynamics, i.e. the cylinder and the wake move in a lateral direction as solid body. Therefore the data obtained in a frame moving with the vibrating cylinder would be the same as those obtained in the case of a non-vibrating cylinder. this means that in a laboratory frame the intermittency factor profile would be $\gamma = \gamma_0\ (y+y_0)$ and the profile of exponent μ would be $\mu = \mu_0[\gamma_0(y+y_0)]$ where γ_0 and μ_0 are data obtained behind the non-vibrating cylinder. Therefore it is convenient to use two-stage averaging. At the first stage the data could be averaged over a time interval much smaller than the timescale of a cylinder movement. At the second stage the p.d.f. of the cylinder position $P(y_0)$ must be used to average all data, i.e.

$$R_{\epsilon\epsilon} \sim \int r^{-\mu_0[\gamma_0(y+y_0)]} P(y_0)\,\mathrm{d}y_0. \tag{27}$$

Equation (27) is basically the same as (8). Similarly we have

$$R_{\epsilon\epsilon} \sim r^{-\mu_0[\gamma_0(y+y_{0\max})]}$$

if r tends to zero. Here $y_{0\max}$ is a maximal value of y_0. If y is excluded from the equations

$$\mu_0 = \mu[\gamma_0(y+y_0)], \quad y = \int \gamma_0(y+y_0)\,P(y_0)\,\mathrm{d}y_0,$$

then a dependence μ on γ could be obtained. It is evident that such a dependence does not need to be the same as presented in figure 15. However, even in this case there is the possibility that all exponents in the inertial subrange power laws could depend on one parameter since exponents $\mu_{1.5}$ and μ_2 are linearly dependent on μ (see figure 16).

It could be concluded from this example that the variability of exponent μ is an alternative in nature. It seems that proof of such variability could be based on comparing data in figures 15 and 17: values of exponent μ obtained from conventionally and conditionally averaged data are different. Thus it seems that one of the basic conclusions of multifractal theory (Parisi & Frisch 1985) is confirmed by the present study.

On the other hand it is seen in figure 23 that there is some kind of direct interaction between dissipation fluctuations and movement of eddies with scales much larger than the Kolmogorov scale. This interaction could be one of the causes of random variability of exponent μ. Such an interaction is ignored in the multifractal model,

since it is assumed that the random variability of all exponents is caused by singularities of solutions of the inviscid Navier–Stokes equations. The present experiments neither confirm nor contradict this idea.

The final manuscript was prepared while A. A. P. was a Senior Research Fellow at the NASA/Stanford Center for Turbulence Research. The authors express sincere gratitude to CTR for support and to Professor P. Bradshaw, Drs S. S. Veeravalli and S. Belcher for comments on the draft.

REFERENCES

ANSELMET, F., GAGNE, Y., HOPFINGER, E. J. & ANTONIA, R. A. 1984 High-order velocity structure functions in turbulent shear flows. *J. Fluid Mech.* **140**, 63–89.

ANTONIA, R. A. 1981 Conditional sampling in turbulence measurements. *Ann. Rev. Fluid Mech.* **13**, 131–151.

ANTONIA, R. A., BROWNE, L. W. B. & SHAH, D. A. 1988 Characteristics of vorticity fluctuations in a turbulent wake. *J. Fluid Mech.* **189**, 349–365.

ANTONIA, R. A., SATYAPRAKASH, B. R. & HUSSAIN, A. K. M. F. 1982 Statistics of fine-scale velocity in turbulent plane and circular jets. *J. Fluid Mech.* **119**, 55–89.

ARGOUL, F., ARNEODO, A., GRASSEAU, G., GAGNE, Y., HOPFINGER, E. J. & FRISCH, U. 1989 Wavelet analysis of turbulence reveals the multifractal nature of the Richardson cascade. *Nature* **338**, 51–53.

BACRY, E., ARNEODO, A., FRISCH, U., GAGNE, Y. & HOPFINGER, E. J. 1989 Wavelet analysis of fully developed turbulence data and measurements of scaling exponents. In *Turbulence and Coherent Structures* (ed. M. Lesieur & O. Métais). Kluwer.

BATCHELOR, G. K. 1953 *The Theory of Homogeneous Turbulence.* Cambridge University Press.

BROWNE, L. W. B., ANTONIA, R. A. & SHAH, D. A. 1987 Turbulent energy dissipation in a wake. *J. Fluid Mech.* **179**, 307–326.

CHAMPAGNE, F. H. 1978 The fine-scale structure of the turbulent velocity field. *J. Fluid Mech.* **86**, 67–108.

CHAMPAGNE, F. H., PAO, Y. H. & WYGNANSKI, I. J. 1976 On the two-dimensional mixing region. *J. Fluid Mech.* **74**, 209–250.

CHHABRA, A. B., Meneveau, C., Jensen,. R. V. & Sreenivasan, K. R. 1989 Direct determination of the $f(\alpha)$ singularity spectrum and its application to fully developed turbulence. *Phys. Rev.* A **40**, 5284–5924.

FOSS, J. F. & WALLACE, J. M. 1989 The measurements of vorticity in transitional and fully developed turbulent flows. In *Advances in Fluid Mechanics Measurements* (ed. M. Gad-el-Hak). Lecture Notes in Engineering, vol. 45. Springer.

FRISCH, U., SULEM, PH. L. & NELKIN, M. 1978 A simple dynamical model of intermittent fully developed turbulence. *J. Fluid Mech.* **87**, 719–737.

GAGNE, Y. & HOPFINGER, E. J. 1979 High order dissipation correlations and structure functions in an axisymmetric jet and plane channel flow. In *Proc. 2nd Symp. Turbulent Shear Flows, Imperial College*, London.

HEDLEY, T. B. & KEFFER, J. F. 1974 Turbulent/non-turbulent decisions in an intermittent flow. *J. Fluid Mech.* **64**, 625–644.

HESKESTAD, G. 1965 A generalized Taylor hypothesis with application for high Reynolds number turbulent shear flow. *Trans. ASME* E: *J. Appl. Mech.* **32**, 735–739.

JENKINS, P. E. & GOLDSCHMIDT, W. W. 1976 Conditional (point averaged) temperature and velocity in heated plane jet. *Phys. Fluids* **19**, 613–617.

KOLMOGOROV, A. N. 1941 Turbulence fine-scale structure in a viscous incompressible fluid at very high Reynolds number. *Dokl. Akad. Nauk SSSR* **30**, 299–303.

KOLMOGOROV, A. N. 1962 A refinement of previous hypothesis concerning the local structure of turbulence in a viscous incompressible fluid at high Reynolds number. *J. Fluid Mech.* **13**, 82–85.

KUZNETSOV, V. R. 1967 Two-point PDF of velocity difference in homogeneous isotropic turbulence. *Prikl. Mat. Mekh.* **31**, 1069–1072.

KUZNETSOV, V. R. 1972 A PDF of passive scalar concentration in turbulent shear flows. *Izv. Akad. Nauk SSSR Mech. Zhid. Gaza* **6**, 85–89.

KUZNETSOV, V. R. 1976 PDF of velocity in an inertial subrange of turbulence spectrum. *Izv. Akad. Nauk SSSR Mech. Zhid. Gaza* **2**, 32–41.

KUZNETSOV, V. R., PRASKOVSKY, A. A. & SABELNIKOV, V. A. 1984 Experimental investigation of intermittency and turbulence fine-scale structure in turbulent shear flows. In *Structure of Gaseous Flames*, Part 2, pp. 21–38. Novosibirsk, ITPM SO AN SSSR.

KUZNETSOV, V. R., PRASKOVSKY, A. A. & SABELNIKOV V. A. 1988 Turbulence fine-scale structure in strongly intermittent shear flows. *Izv. Akad. Nauk SSSR Mech. Zhid. Gaza* **6**, 51–59.

KUZNETSOV, V. R. & RASSCHUPKIN, V. I. 1977 PDF and conditional sampling in turbulent flows. *Izv. Akad. Nauk SSSR Mech. Zhid. Gaza* **6**, 31–37.

KUZNETSOV, V. R. & SABELNIKOV, V. A. 1986 *Turbulence and Combustion*. Moscow: Nauka. (English Transl. Hemisphere, 1990).

LARUE, J. C. & LIBBY, P. A. 1976 Statistical properties of the interface in the turbulent wake of a heated cylinder. *Phys. Fluids* **19**, 1864–1875.

LUMLEY, J. L. 1965 Interpretation of time spectra measured in high intensity shear flows. *Phys. Fluids* **8**, 1056–1062.

MONIN, A. S. & YAGLOM, A. M. 1967 *Statistical Fluid Mechanics*. vol. 2. Moscow: Nauka. (English Transl. MIT Press, 1975).

NOVIKOV, E. A. 1971 Intermittency and scaling in turbulent flows. *Prikl. Mat. Mekh.* **35**, 266–277.

NOVIKOV, E. A. & STEWART, R. W. 1964 Intermittency and dissipation fluctuation spectrum. *Izv. Akad. Nauk SSSr Geogr. Geofiz.* **3**, 408–413.

OBOUKHOV, A. M. 1941 Spectrum of energy of turbulent flow. *Dokl. Akad. Nauk. SSSR* **32**, 22–24.

OBOUKHOV, A. M. 1962 Some specific features of atmospheric turbulence. *J. Fluid Mech.* **13**, 1, 77–81.

PARISI, G. & FRISCH, U. 1985 On the singularity structure of fully developed turbulence. In *Turbulence and Predictability in Geophysical Fluid Dynamics and Climate Dynamics* (ed. M. Ghil, R. Benzi & G. Parisi), pp. 84–87. North-Holland.

PHILLIPS, O. M. 1955 The irrotational motion outside a free turbulent boundary. *Proc. Camb. Phil. Soc.* **51**, 220–229.

POND, S. & STEWART, R. W. 1965 Measurements of characteristics of turbulence finescale structure. *Izv. Akad. Nauk SSSr Fiz. Atmos. Oceana* **1**, 914–919.

PRASKOVSKY, A. A. 1982 Intermittency function measurements. In *Papers of the Third All-Union Conf. on Methods of Aerophysical Investigations*, Part 2, pp. 133–136. Novosibirsk, ITPM.

PRASKOVSKY, A. A. 1983 Measurements of conditionally averaged turbulence characteristics in a plane wake. *Prikl. Mech. Tehn. Fiz.* **6**, 87–94.

SIEBESMA, A. P., TREMBLAY, R. R., ERZAN, A. & PIETRONERO, Z. 1989 Multifractal cascades with interactions. *Physica* A **156**, 613–627.

TOWNSEND, A. A. 1956 *The Structure of Turbulent Shear Flow*. Cambridge University Press.

TSINOBER, A., KIT, E. & DRACOS, T. 1992 Experimental investigation of the field of vorticity gradients in turbulent flows. *J. Fluid Mech.* (in press).

WYNGAARD, J. C. 1968 Measurements of small-scale turbulent characteristics with hot-wires. *J. Sci. Instrum.* **1**, 1105–1108.

YAGLOM, A. M. 1966 Dependence of inertial-subrange characteristics on dissipation fluctuations. *Dokl. Akad. Nauk SSSR* **166**, 49–52.

YAGLOM, A. M. 1981 Turbulence fine-scale structure in atmosphere and ocean (Towards the 40th anniversary of the turbulence fine-scale structure theory). *Izv. Akad. Nauk SSSR Fis. Atmos. Okeana* **17**, 1235–1257.